ELSEVIER

Polymer 40 (1999) 919–925

polymer

Yielding and plastic behaviour of amorphous atactic poly(oxypropylene) under uniaxial compression: an atomistic modeling approach

Seung Soon Jang, Won Ho Jo*

Department of Fiber and Polymer Science, Seoul National University, Seoul 151-742, South Korea

Received 16 January 1998; revised 23 March 1998; accepted 15 April 1998

Abstract

The yielding and plastic behaviour of atactic poly(oxypropylene) (a-POP) was simulated under the uniaxial compression condition using atomistic modelling, and compared with the result under the uniaxial extension condition. Typical stress–strain curves showing yielding and plastic behaviour were obtained under the uniaxial compression condition. It was observed that the stress under uniaxial compression is greater than that under uniaxial extension. This observation suggests that the difference of stress level between the two conditions is not related intrinsically to the structural defects in the sample. When the energetic state of a-POP was analysed by monitoring the change of energy component with strain, it revealed that the change of total energy with strain was governed dominantly by non-bonded interaction, such as van der Waals and Coulombic interaction. The role of Coulombic interaction is more important under compression than under extension.

Keywords: Yielding; Amorphous atactic poly(oxypropylene); Uniaxial compression

1. Introduction

Until the present day, the yielding and plastic behaviour of polymers has not been thoroughly understood at the microstructural level. Why the nature of yielding and plastic behaviour of amorphous polymers still remains veiled, is attributed to the shortcomings involved in the experimental and theoretical approach. In the experimental approach, microscopic and/or macroscopic defects in samples can mislead the conclusion, whereas in the theoretical approach, excessive assumptions introduced for simplifying mathematical calculation may reduce the predictability of the theory for physical properties. An atomistic modelling approach makes a rigorous description of polymeric system possible, by removing and/or controlling such shortcomings mentioned above. Indeed, in recent years, the atomistic modelling of polymers has provided us with a lot of useful information for predicting and interpreting the mechanical properties of various polymers [1–9].

In order to simulate mechanical properties of amorphous polymers, a molecular mechanics technique [10,11] was adopted in this work. Using molecular mechanics with a parameterized force field, the procedure consisting of deformation and relaxation was implemented in a simulation cell, whose structure was equilibrated beforehand by a molecular dynamics technique. In some papers, instead of molecular mechanics, a molecular dynamics technique was used for the mechanical simulation of polymers [7,8,12–14]. Although molecular dynamics has an advantage that it can directly examine the temperature effect on the deformation process, it is very time-consuming when carried out with a full atomistic model. On the other hand, molecular mechanics requires relatively short computing time without a significant loss of its predictability.

It is well known that atactic poly(oxypropylene) (a-POP, $-(CH_2CH(CH_3)O)_n-$) can be synthesized from racemic mixtures of propylene oxide in the presence of KOH catalyst [15], and has often been used as a soft segment in the synthesis of polyurethane elastomers. Its flexibility and low glass transition temperature ($T_g = 198$ K) [16] imparts a good elastic recovery to polyurethane. In addition, a-POP is strongly resistant to hydrolysis and has a low ability to crystallize [17]. In this study, the yielding and plastic deformation of amorphous a-POP was simulated under the uniaxial compression condition using an atomistic modelling technique, and the results were compared with those [18] obtained under uniaxial extension.

* Corresponding author.

0032-3861/98/$ - see front matter
PII S0032-3861(98)00311-5

2. Model and simulation

Full atomistic models of a-POP with 90 repeating units (902 atoms) were prepared. In the simulation, the commercial modelling software, *Cerius2* (Molecular Simulation Inc.) was used. The initial conformation of the a-POP chain in the cell was generated in a cubic cell with periodic boundary conditions by the RIS method, as shown in Fig. 1. The initial density, 1.3 g/cm^3, was optimized to the value comparable with the experimental one. As the initial structure has very high energy and is far from the mechanical equilibrium state due to overlap of van der Waals spheres, the structure should be relaxed and optimized as follows. The amorphous cell was equilibrated at 1000 K for 50 ps, and then at 298.15 K for 50 ps by the canonical ensemble (NVT) molecular dynamics with a time step of 1 fs. Thereafter, in order to obtain an isotropic stress state, the isothermal–isobaric ensemble (NPT) molecular dynamics was carried out at 298.15 K for 100 ps, and finally cell optimization was performed by molecular mechanics.

The universal force field [19] was used to calculate potential energies of atoms, and the charge equilibration method [20] was used to assign partial charges to atoms. The Ewald method [21] was used to calculate the long-range interactions, such as the van der Waals and Coulombic interactions. The total potential energy (E_{total}) of the system is calculated by using Eq. (1):

$$E_{\text{total}} = E_{\text{b}} + E_{\theta} + E_{\phi} + E_{\text{vdW}} + E_{\text{Coulomb}} + E_{\text{inversion}} \quad (1)$$

where E_{b} is the bond stretching energy, E_{θ} is the valence angle bending energy, E_{ϕ} is the dihedral angle torsion energy, E_{vdW} is the van der Waals interaction energy, E_{Coulomb} is the Coulombic interaction energy, and $E_{\text{inversion}}$ is the inversion energy. The details of energy function were given by Rappé et al. [19] After equilibration and optimization, a-POP cell was uniaxially compressed. The cell was compressed by 0.2% of the initial cell dimension, and then relaxed by the energy minimization using conjugate gradient algorithm. This procedure was repeated until the strain reached 15%.

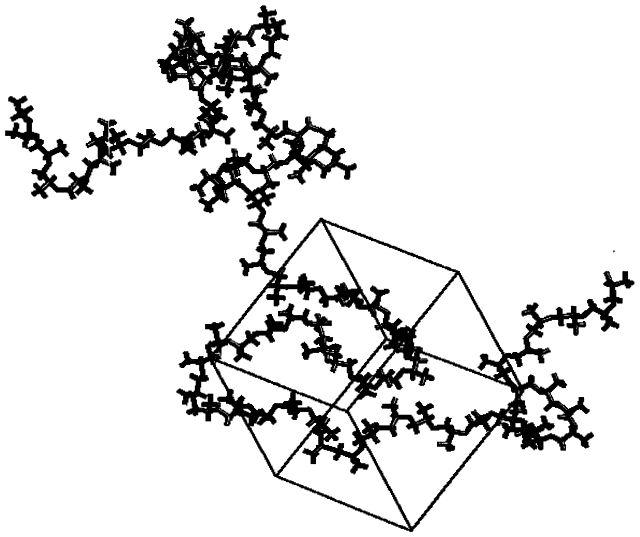

Fig. 1. Typical structure of an amorphous a-POP cell.

3. Results and discussion

3.1. Validation of simulation

In order to obtain reliable mechanical properties of the polymer from molecular simulation, the cell dimension should be larger than the persistence length of the polymer. If the cell dimension is smaller than the persistence length, the simulation may not properly describe the mechanical behaviour, because movement of a segment influences itself through the periodic boundary conditions through its self-replica. The average dimension parameters of optimized cells (−20 Å) were three times larger than the persistence length of a-POP (5.6 Å) [18]. The average cell density was 1.009 ± 0.018 g/cm^3 comparable with the experimental one [15] (0.998–1.097 g/cm^3). As another criterion to determine whether the energetic state of the cell properly describes the state of the real material, and whether the force field adopted is suitable for the material, the solubility parameter was calculated [18.90 ± 0.32 (J/cm^3)$^{1/2}$]. This value is in good agreement with 18.9 (J/cm^3)$^{1/2}$ predicted by the group contribution theory [22], and with 15.4–20.3 (J/cm^3)$^{1/2}$ obtained from experiments [23,24].

It is important to ascertain whether the simulated structure in the cell is amorphous. The fundamental difference between the crystalline and amorphous states is the existence of long-range order found in the former, which is absent in the latter. The pair correlation function, also referred to as the radial distribution function, can describe this long-range order [25]. The pair correlation function is defined as the probability of finding a pair of all kinds of atoms in the system at a distance r apart, relative to the probability expected for a completely random distribution at the same density. The total pair correlation function for a cell is shown in Fig. 2. From the fact that the $g(r)$ approaches the value of 1 at $r > 3$ Å, it is obvious that there exists no long-range order in the cell, and hence, this structure shows a typical feature of the amorphous state. The peaks in the regime of $r < 3$ Å are due to the atomic connectivity in repeating units of a-POP.

The molecular weight of a-POP simulated in this study may be thought of as relatively small. It has been reported that mechanical properties of the polymer are dependent upon its molecular weight. However, it should be noted that the molecular mechanics technique, as a quasi-static method, removes the molecular weight effect on the mechanical properties of the polymer due to the following reasons. Firstly, the model used in this simulation does not have any structural defect which may initiate the fracture. Secondly, the chain scission is assumed not to occur, since

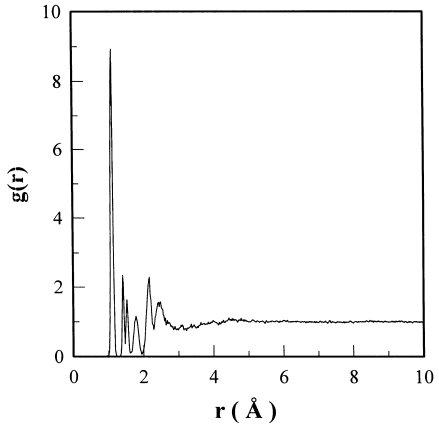

Fig. 2. The total pair correlation function of the undeformed a-POP chain.

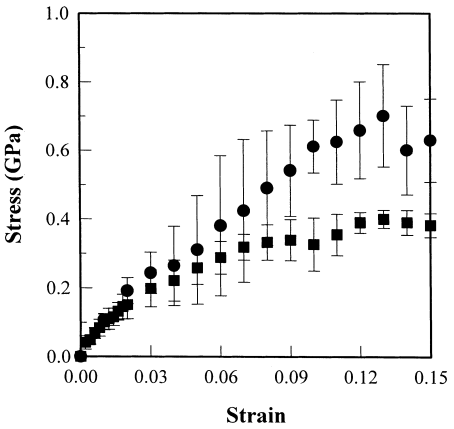

Fig. 3. The stress–strain curve of a-POP: (■) under uniaxial extension condition; (●) under compression condition.

the force field used in this simulation does not allow the bond breakage. Thirdly, because the strain is imposed to the cell very slowly at 0 K, as mentioned in the previous section, the polymer chain in the cell has enough time to be relaxed without sudden chain slippage, that depends strongly on the entanglement molecular weight of the polymer. Therefore, the simulation in this study is progressed in an ideal condition, which excludes the effects of structural defect and molecular weight on mechanical properties.

3.2. Yielding and plastic behaviour under uniaxial extension/compression

The uniaxial compression was imposed on the cell, thereby a stress–strain curve typically observed in experiments was obtained and compared with that under uniaxial extension [18], as shown in Fig. 3. Under both conditions, elastic responses were the same up to the strain of 2%. Since stress begins to deviate from the straight line, with an initial slope at about 2% strain in both cases, it is clear that the plastic deformation begins to occur after 2% strain. It is also observed that the stress under compression is larger than that under extension, and that the difference of stress at the same strain between extension and compression becomes greater up to the apparent yield point (−13% strain), defined as a maximum load point. This feature of the stress–strain curve is in agreement with experimental results [26–28]. Experiments show that the stress under uniaxial-compression is larger than that under uniaxial extension. The reason has often been explained by considering the presence of macrostructural and/or microstructural defects in the sample. In other words, it is because the crazing easily developed from defects under the uniaxial extension condition does not occur under the uniaxial compression condition. Our simulation results also show the higher stress level under the uniaxial compression condition as compared with the uniaxial extension condition, although there is no structural defects in the simulation cell, indicating that the difference of stress level between two conditions is not related intrinsically to the structural defects in the sample.

The change in structure of a-POP was investigated in an attempt to correlate the characteristic change in structure with the yielding and plastic behaviour of a-POP. The change in chain dimensions, such as the end-to-end distance and the radius of gyration of a-POP with strain, is shown in Fig. 4. Obviously, the change in chain dimensions is negligible under both conditions. Fig. 5 shows the change of bond orientation function with the strain. Bond orientation function is given by

$$P_2 = \tfrac{1}{2}[3\langle\cos^2\theta\rangle - 1] \quad (2)$$

where θ is the angle between each bond and an axis. The initial value of P_2 close to zero indicates that bond orientation of a-POP is random in the undeformed state. As the strain increases, the value of $P_{2\parallel}$ parallel to the strain direction slightly increases linearly under the uniaxial extension condition, whereas that of $P_{2\parallel}$ slightly decreases linearly under the uniaxial compression condition. In any case, however, the change in the orientation function is very small up to 15% strain, indicating that the a-POP chain remains almost randomly oriented after plastic deformation. It is generally known that extension/compression causes anisotropy in the structure by reorienting the chains. However, the strain-induced structural anisotropy in the amorphous phase is far slower than in the crystalline phase [29,30], which is consistent with the result of this simulation.

The change in chain conformation with strain was analysed in this study. In order to investigate the change of chain conformation, the distribution of dihedral angles in the a-POP backbone chain was calculated at various strains under the uniaxial extension/compression conditions. There exists three kinds of dihedral angles in an a-POP backbone chain, such as CC*OC(ϕ_1), C*OCC* (ϕ_2) and OCC*O (ϕ_3) shown in Fig. 6a, and the distribution of these dihedral angles of the undeformed state is shown in Fig. 6b. In order to analyse the conformational change

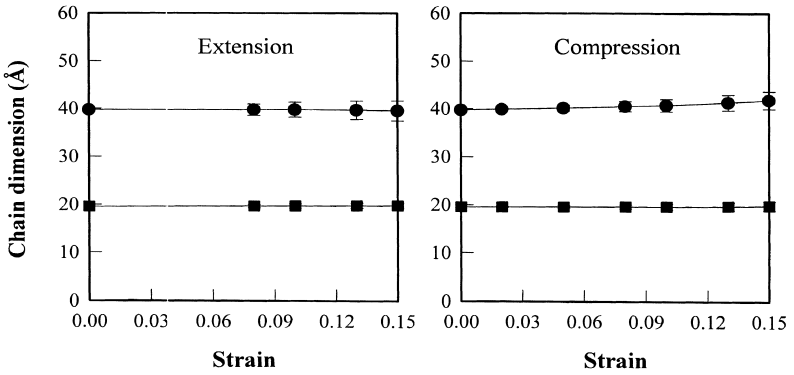

Fig. 4. The change of chain dimension with strain for a-POP. The symbols (●) and (■) represent end-to-end distance and radius of gyration, respectively.

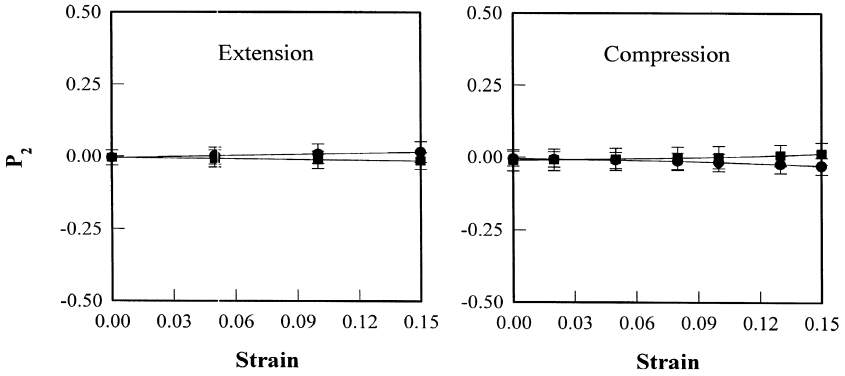

Fig. 5. The change of bond orientation function with strain for a-POP. The symbols (●) and (■) represent $P_{2\parallel}$ and $P_{2\perp}$, respectively.

quantitatively, the change in amount of each dihedral angle having *trans* state ($2n\pi - \pi/6 < \phi < 2n\pi + \pi/6$, $n = 0, 1, 2, \ldots$) was calculated with the strain. Fig. 7 shows that the amount of dihedral angles having *trans* state remains almost unchanged with the strain under both conditions. Therefore, it is concluded that the chain conformation does not change significantly with the strain, and hence, the yielding and plastic behaviour does not originate from the change in the chain conformation. Generally, the volume of glassy polymer whose Poisson's ratio is smaller than 0.5 increases with the strain under uniaxial extension, and decreases under uniaxial compression. In this study, the change in cell volume with the strain was monitored under compressiosn and compared with that under extension, as shown in Fig. 8. Under the uniaxial compression condition, the change in cell volume is more complicated than that under the uniaxial extension condition, where the volume increases monotonously with the strain. Under the uniaxial compression condition the cell volume decreases in the elastic region, as expected from the Poisson's ratio. Thereafter, the cell volume remains almost constant up to 10% strain, and then increases with the strain. Fig. 8 shows that the Poisson's ratio of a-POP remains almost constant under uniaxial extension, whereas, under uniaxial compression, it increases up to almost 0.5 and levels off in the range of 3–10% strain, and then increases again. As the mass of the system is conserved during simulation, the change in cell volume must occur due to

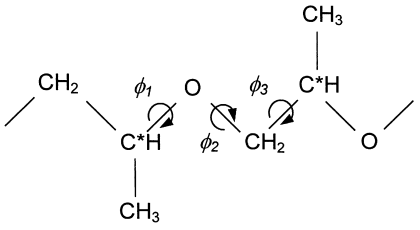

(a)

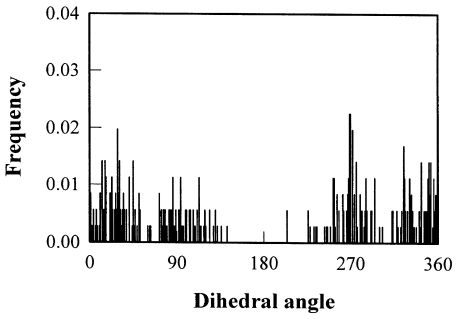

(b)

Fig. 6. The definition of dihedral angles in the a-POP backbone chain (a), and their distribution (b).

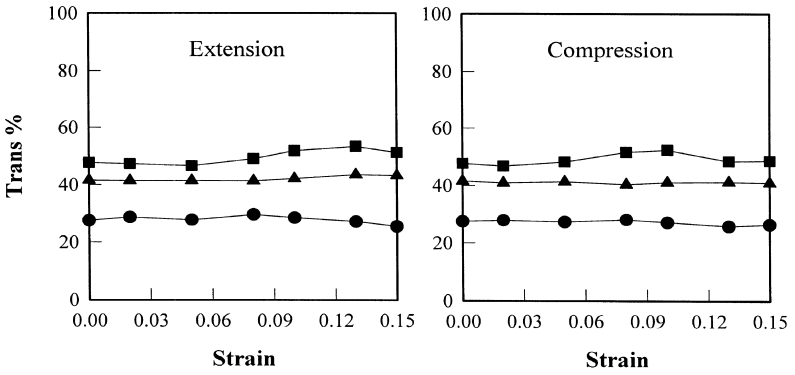

Fig. 7. The change in amount of each dihedral angle having *trans* state with strain for a-POP: (●) CCOC; (■) C*OCC*; (▲) OCC*O.

the change of free volume in the cell. In our previous paper [18], we measured the Voronoi volume, which corresponds to the free volume, and its distribution under extension. The result showed that the size of the Voronoi volume is not as large as microscopic voids. Therefore, it is obvious that the increase of free volume in the polymer is suppressed under the uniaxial compression condition rather than under the uniaxial extension condition. This difference of volume change between two conditions can be related to the difference between stress levels under these two conditions, as shown in Fig. 3. As the cell volume of a-POP is rather contracted under the uniaxial compression condition, the hydrostatic pressure under compression becomes higher than that under extension, and thus, the stress component in the direction of compression is greater than that in the direction of extension. This explanation for the nature of the difference between extension and compression is also supported by Crist [31].

The energetic state of a-POP was analysed by monitoring the change of each energy component with strain. The changes of energy components under both conditions show almost the same trend as shown in Fig. 9. The change of total energy with strain seems to be governed dominantly by non-bonded interaction, such as van der Waals and Coulombic interactions, the former being far more dominant than the latter. Another feature to note is that the role of Coulombic interaction is more important under compression than under extension because, at the same strain, the cell under compression is more closely packed than under extension, and thus, the Coulombic attraction between methylene hydrogen and ether oxygen, depending strongly upon the inter-atomic distance, becomes more important under the uniaxial compression condition than under the uniaxial extension condition. In order to specify the role of van der Waals interaction, the supplementary simulation was carried out using a modified force field that consists of only a bond stretching and a van der Waals interaction component, a-POP chain being regarded as a self-avoiding and non-intersecting chain without restriction from the valence or dihedral angles. Fig. 10 shows the stress–strain curves under uniaxial extension/compression condition using two different force fields: one is the universal force field consisting of all energy components, and the other is the modified force field. First of all, it is very suggestive that the yielding and plastic behaviour appears in all the stress–strain curves. Particularly, the elastic response under each condition is identical regardless of the force field used, and the trend of curves is very similar. Considering the result shown in Fig. 9, it may be concluded that the yielding and plastic behaviour of a-POP is attributed mainly to the van der Waals interaction.

Another point to be noteworthy is that Fig. 10 shows a different stress level in the stress–strain curve under different force fields. Under the uniaxial extension condition, the stress level using the modified force field is lower than that using the universal force field, whereas under the uniaxial compression condition the stress levels are almost the same within their standard deviations. Although it is reasonable to consider that the valence angle bending and dihedral angle torsion energies of the universal force field play an important role under the uniaxial extension condition rather than under the uniaxial compression condition; future work is necessary to explain these results in detail.

In summary, the non-bonded interaction, such as the van

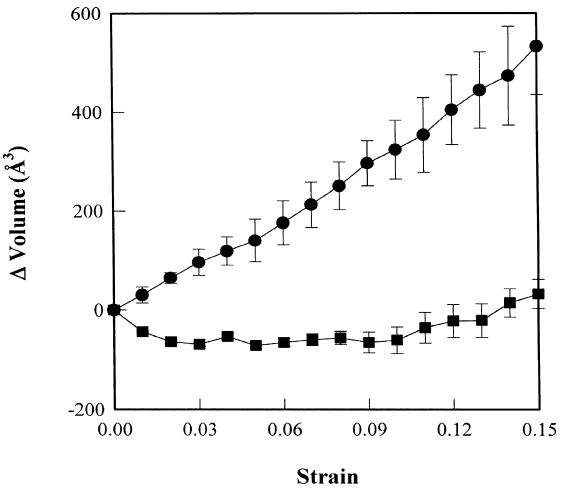

Fig. 8. The change of cell volume with strain for a-POP: (●) under extension; (■) under compression.

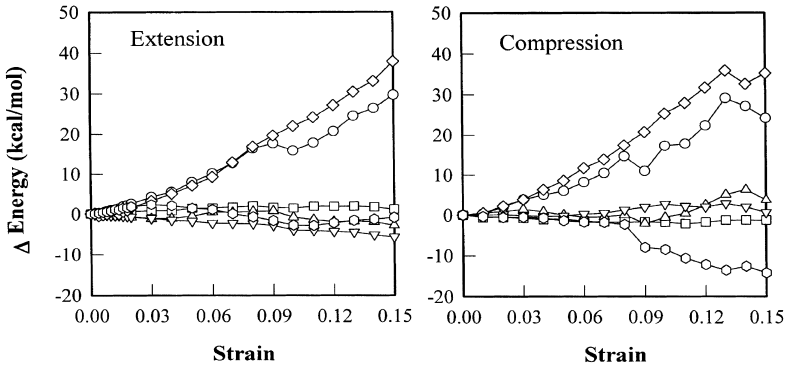

Fig. 9. The changes of energy components for a-POP: (○) total energy; (□) bond stretching; (△) valence angle bending; (▽) dihedral angle torsion; (◇) van der Waals interaction; (⬭) Coulombic interaction.

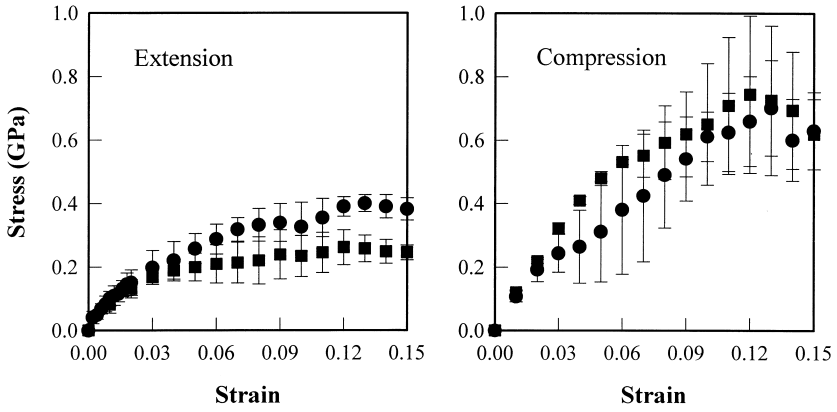

Fig. 10. The stress—strain curves of a-POP obtained using different force field: (●) universal force field; (■), modified force field.

der Waals interaction, is sensitive to strain, whereas the chain conformation does not change significantly with strain, because the van der Waals interaction calculated by the Lennard–Jonnes 12-6 function is strongly dependent on inter-atomic distance, whereas the chain conformation is less sensitive to the inter-atomic distance. Therefore, it is concluded that the contribution of the van der Waals interaction to the yielding and plastic behaviour of a-POP is dominant.

4. Conclusions

Using atomistic modelling, the yieldidg and plastic behaviour of a-POP was simulated under the uniaxial compression condition, and compared with the result under the uniaxial extension condition for the first time. The density and energetic state of the a-POP structure was in agreement with that obtained from experiments. Using a molecular mechanics technique, stress–strain curves were obtained, and their features were in good agreement with those from experiments. The lower stress level under the uniaxial extension condition as compared with the stress under uniaxial compression was observed in the simulation, although there is no structural defects in the simulation cell. This suggests that the difference in the stress level between the two conditions is not related intrinsically to the structural defects in the sample. From various analyses of chain conformation of a-POP, it is obvious that the yielding and plastic behaviour of a-POP requires no specific change in chain conformation under both the uniaxial extension and compression conditions. The change of total energy with strain seems to be governed by non-bonded interactions, such as van der Waals and Coulombic interactions, the former being far more dominant than the latter. The role of Coulombic interaction is more important under compression than under extension, because the cell under compression is more closely packed than that under extension.

References

[1] Mott PH, Argon AS, Suter UW. Phil Mag 1993;67:931.
[2] Gusev AA, Zehnder MM, Suter UW. Macromolecules 1994;27:6153.
[3] Argon AS, Bulatov VV, Mott PH, Suter UW. J Rheol 1995;39:377.
[4] Marcel U, Tomaselli M, Richard RE, Suter UW. Macromolecules 1996;29:2909.
[5] Fan CF, Cagin T, Chen ZM, Smith KA. Macromolecules 1994;27:2383.
[6] Fan CF. Macromolecules 1995;28:5215.

[7] Raska T, Niemelä S, Sundholm F. Macromolecules 1994;27:5751.
[8] Ogura I, Yamamoto T. Polymer 1995;36:1375.
[9] Vasudevan VJ, McGrath JE. Macromolecules 1996;29:637.
[10] Burkert U, Allinger NL. Molecular mechanicy. Washington, DC: ACS, 1982.
[11] Rappé AK, Casewit CJ. Molecular mechanics across chemistry. Sausalito, CA: University Science Books, 1997.
[12] Brown D, Clarke JHR. Macromolecules 1991;24:2075.
[13] Brown D, Clarke JHR. Comput Phys Commun 1991;62:360.
[14] McKechnie JI, Haward RN, Brown D, Clarke JHR. Macromolecules 1993;26:198.
[15] Abe A, Hirano T, Tsuruta T. Macromolecules 1979;12:1092.
[16] Brandrup J, Immergut EH. Polymer handbook, 3rd edn. New York: Wiley, 1989.
[17] Hepburn C. Polyurethane elastomers, 2nd edn. New York: Elsevier, 1992.
[18] Jang SS, Jo WH. Macromol Theory Simul. Submitted for publication.
[19] Rappé AK, Casewit CJ, Colwell KS, Goddard III WA, Skiff WM. J Am Chem Soc 1992;114:10024.
[20] Rappé AK, Goddard III WA. J Phys Chem 1991;95:3358.
[21] Karasawa N, Goddard III WA. J Phys Chem 1989;93:7320.
[22] van Krevelen DW, Hoftyzer PJ. Properties of polymers — their estimation and correlation with chemical structure. New York: Elsevier, 1976.
[23] Becker RZ. Phys Chem 1977;258:953.
[24] Lee WA, Sewell JH. J Appl Polym Sci 1968;12:1397.
[25] Allen MP, Tildesley DJ. Computer simulation of liquids. New York: Oxford University Press, 1987.
[26] Ibrahim N, Shinizaki DM, Sargent CM. Mater Sci Engng 1977;30:175.
[27] Spitzig WA, Richmond O. Polym Engng Sci 1979;19:1129.
[28] Bauwens C-C, Bauwens J-C, Homés G. J Mater Sci 1972;7:176.
[29] Samuel RJ. Structured polymer properties. New York: Wiley, 1974.
[30] Ward IM, Hadley DW. An introduction to the mechanical properties of solid polymers. New York: Wiley, 1993.
[31] Crist B. In: Cahn RW, Haasen P, Kramer EJ, editors. Materials science and technology, vol. 12: structure and properties of polymers. Weinheim: VCH, 1993.